PLOS COMPLEX SYSTEMS

RESEARCH ARTICLE

Inferring leader-follower behavior from presence data in the marine environment: A case study on Reef Manta Rays

Juan Fernández-Gracia[1*], **Jorge P. Rodríguez**[1], **Lauren R. Peel**[2,3,4], **Konstantin Klemm**[1], **Mark G. Meekan**[5,6], **Víctor M. Eguíluz**[1]

1 Instituto de Física Interdisciplinar y Sistemas Complejos IFISC (CSIC-UIB), Palma de Mallorca, Spain, **2** Australian Institute of Marine Science, Indian Ocean Marine Research Centre (IOMRC), University of Western Australia, Crawley, Australia, **3** Save Our Seas Foundation - D'Arros Research Centre (SOSF-DRC), Amirantes, Republic of Seychelles, **4** The Manta Trust, Corscombe, United Kingdom, **5** Oceans Institute, University of Western Australia, Crawley, Australia, **6** Ocean Sciences and Solutions Applied Research Institute, Neom Corp, Saudi Arabia

* juanf@ifisc.uib-csic.es

OPEN ACCESS

Citation: Fernández-Gracia J, Rodríguez JP, Peel LR, Klemm K, Meekan MG, Eguíluz VM (2025) Inferring leader-follower behavior from presence data in the marine environment: A case study on reef manta rays. PLoS Complex Syst 2(10): e0000073. https://doi.org/10.1371/journal.pcsy.0000073

Editor: Timothy Saunders, University of Warwick, SINGAPORE

Received: December 12, 2024

Accepted: September 20, 2025

Published: October 9, 2025

Peer Review History: PLOS recognizes the benefits of transparency in the peer review process; therefore, we enable the publication of all of the content of peer review and author responses alongside final, published articles. The editorial history of this article is available here: https://doi.org/10.1371/journal.pcsy.0000073

Data availability statement: The code is available through the github repository in [45].

Abstract

Social interactions are fundamental in animal groups, including humans, and can take various forms, such as competition, cooperation, or kinship. Understanding these interactions in marine environments has been historically challenging due to data collection difficulties. However, advancements in acoustic telemetry now enable the remote analysis of such behaviors. This study proposes a method to derive leader-follower networks from presence data collected by a single acoustic receiver at a specific location.

Using the Kolmogorov-Smirnov distance, the method analyzes lag times between consecutive presences of individuals to infer directed relationships. Tested on simulated data, it was then applied to detection data from acoustically tagged reef manta rays (*Mobula alfredi*) frequenting a known site. Results revealed temporal patterns, including circadian rhythms and burst-like behavior with power-law distributed time gaps between presences.

The inferred leader-follower network highlighted key behavioral patterns when compared to an appropriate random null model: females followed males more often than expected, males showed stronger but fewer associations with specific females, and smaller individuals were less consistent in following others than larger ones. These findings align with ecological insights, revealing structured social interactions and providing a novel framework for studying marine animal behavior through network theory.

Author summary

Understanding social structures in animal populations is critical for advancing both ecological theory and conservation strategies. This study introduces a novel approach to

The acoustic telemetry data supporting this research are sensitive and not available publicly. Data are available to qualified researchers upon reasonable request to the D'Arros Research Centre at contact-drc@saveourseas.com.

Funding: VME and JFG acknowledge partial support from projects MISLAND (PID2020-114324GB-C22) and CSxAI (PID2024-157526NB-I00). JPR was supported by Govern de les Illes Balears through the Vicenç Mut program. Fieldwork and data collection was funded by the Save Our Seas Foundation (SOSF) and supported by The Manta Trust and SOSF – D'Arros Research Centre (SOSF-DRC). The funders had no role in study design, data collection and analysis, decision to publish, or preparation of the manuscript.

Competing interests: The authors have declared that no competing interests exist.

infer leader-follower interactions among animals using only presence data, demonstrated through reef manta rays (*Mobula alfredi*). By leveraging statistical methods based on the Kolmogorov-Smirnov distance, the methodology identifies directional interactions from observed temporal patterns in presence data. The approach is validated using synthetic datasets and applied to field data, uncovering directional patterns in manta ray behavior, including sex- and size-dependent following dynamics.
This interdisciplinary work combines tools from statistical physics, network science, and behavioral ecology. The findings provide insights into the social organization of reef manta rays, the structures of which may be monitored over time in order to detect anthropogenic-impact-driven change. Moreover, the methodology is generalizable, offering a robust framework for studying interactions across a wide range of systems where traditional observational methods are impractical. This research contributes to the growing understanding of how complex systems operate in ecological contexts and beyond.

1. Introduction

Social interactions among animals mediate many processes, such as the transmission of information [1,2] or diseases [3]; collective behavior [4–6] (flocking [7], social learning [8], predator avoidance [9], cooperative foraging [10]); selection of phenotypes [11]; mating [10]; or the emergence and maintenance of cooperation [10,12]. The structure of these social interactions as a whole is typically studied with the methods from network theory [13], which have recently and increasingly been applied to animal groups [1–10,14] and represent a promising tool in the field of movement ecology [15].

The first step of studying these interactions involves finding or collecting the data that describe them, before the underlying networks can be extracted in a meaningful and statistically significant way. For humans, the availability of large amounts of digital traces (notably, call detail records and social media accounts [16]) and the ease with which they can be accessed, has facilitated the detailed statistical description of human interactions. Tracking animal social systems [17] in a similar manner, however, has remained a challenge, given the difficulties associated with collecting a sufficient amount of data from the network of interest. This is particularly true in the marine environment, where the large and three-dimensional nature of animal movements imposes logistical, technological and financial constraints on data collection capacities.

Traditionally, the collection of presence data in the marine environment relied on techniques that were applied within discrete sampling periods (e.g. photo-identification [18] or capture-mark-recapture [19,20]). This temporal limitation restricted the extent to which social interactions between sampled individuals could be considered. Recent advances in the field of acoustic telemetry, however, have since provided a means to overcome these issues, allowing the movement and residency patterns of marine fauna to be monitored continuously, and over long periods of time (up to ten years).

In studies using passive acoustic telemetry, acoustic tags that emit a unique sound signal are externally attached to [21], or surgically implanted into [22], study animals. These tags are subsequently detected by acoustic receivers placed at specific locations within the study area (collectively, an acoustic array), and the timestamp of each detection is logged by the devices from which data can be downloaded at a later date. Acoustic arrays and tagging programs have been established worldwide [23–25], and the frequency of their use is increasing as the affordability of the required equipment improves [23,26]. While the primary motivation of

such studies is often to obtain spatial data to inform the development of conservation measures [21,23,27], the potential to use these presence data to examine leader-follower behavior in marine species is yet to be extensively explored.

Leadership behavior has been reported in many animal groups, including insects (e.g. ants) and birds (e.g. migrating storks), and has been found to be of paramount importance in achieving coordination among individuals [28–30]. Should a population lack clear leaders or a hierarchical structure [31], individuals may have preferences on whom they should interact with, subsequently modifying the strength of the social interaction. Additionally, interactions within a social network may not be reciprocal, generating directionality in the flow of information. This allows for the introduction of focal individuals and their leading and following connections, such that the focal individuals' dynamics are coupled with that of its leaders, while that of its followers are coupled with the focal individual's.

Within a typical social network, individuals are represented by nodes, and the interactions recorded between them are represented by connections (or edges). The power of networks to represent social interactions lies within the ability to characterize edges relative to the type of interaction that has occurred. Interactions can be symmetrical, representing exchanges from one peer to the other and vice versa, or directed, originating from a source towards a target. In this sense, leadership behavior can be examined with network tools, too, assuming that the sources represent leaders and the targets represent followers. However, appropriate methods for detecting these asymmetric relations are currently lacking.

Several social network inference methods exist in the literature that are well suited for acoustic telemetry data [14,32–38]. The majority of these rely on detecting the co-occurrence of individuals, and thus have the problem of the Gambit of the group (GoG [14]). That is, every pair of animals observed in the same group is treated as having interacted with one another, although this might appear due to coincidence in visitation patterns and not social affiliation. Early analytical methods also required an appropriate temporal window to be defined, within which co-occurrences were considered [36–39]. This restriction, and that of the GoG, was resolved by the introduction of the 'GMMevents' method by Psorakis and collaborators [32,33]. These methods allowed researchers to investigate the complex social structure of different animal groups, uncovering their relation to individual characteristics, such as sex, size, personality or genetic traits [11,34,40,41].

Here, we aim to develop an analytical method to provide evidence of leader-follower behaviors from acoustic telemetry data, alongside estimates for the statistical significance of the observed interactions. We first describe a novel method for extracting leader-follower interactions from established social networks. We then apply this method to real-world presence data collected for reef manta rays (*Mobula alfredi*) at a single location using passive acoustic telemetry. Reef manta rays present an ideal study species for work of this nature for a number of reasons: (1) they show repeated and prolonged visitation to key sites on coral reefs known as cleaning stations, where individual mantas socialize, and cleaner fishes remove parasites from their bodies [42]; (2) individuals are long-lived and can be accurately identified from unique pigmentation patterns displayed on their bodies throughout their lifetime [18,43]; (3) reef manta rays exhibit two distinct sexes and the size of an individual can be used as a proxy for its maturity status, allowing leader-follower behaviors to be considered relative to these biological traits [44]. Finally, we discuss the applicability of this novel analysis procedure to existing acoustic telemetry datasets, and the potential for future studies of this kind to improve our understanding and management of the complex interplay between ecological processes and environmental change.

2. Materials and methods

All the methods described here have been implemented computationally using Python 3 and are available through the repository in Ref [45].

2.1. Ethics statement

Field research in Seychelles was approved by, and conducted with the knowledge of, the Seychelles Bureau of Standards, the Seychelles Ministry of Environment, Energy and Climate Change.

2.2. Leader-follower interactions from presence data

We propose a measure for quantifying leadership from time series captured for multiple acoustically tagged individuals around a single acoustic receiver. In particular, our method is relevant for examining the collective movement patterns of entities, be it active matter, robots, humans or animals, where presence data of individuals has been recorded at a specific location.

The data for each individual consists of an ordered set of timestamps at which the individual is located in the vicinity of that particular location. In order to infer if individual A typically follows individual B, we hypothesize that the time delay, or lag time, between the consecutive detection of first A and then B will be longer than the reverse (*i.e.* the consecutive times of detecting B followed by A). This hypothesis builds on the idea that if individual A tends to follow individual B, then the movement of A is, to some extent, conditional on the prior movement of B. Therefore, we expect that when B moves first and A follows, the time delay between their detections will be relatively short, reflecting coordinated movement. Conversely, when A moves first and B follows (which would be less typical if A is the follower), their detections would not show the same tight coordination, leading to a longer lag time. In this way, comparing the lag times in both directions provides a proxy for asymmetries in their movement dependencies. We therefore extract the lag times for B followed by A, $\{t_{AB}\}$, and A followed by B, $\{t_{BA}\}$, and their corresponding distributions $p_{AB}(t)$ ($p_{BA}(t)$), such that $p_{AB}(t)dt$ ($p_{BA}(t)dt$) measures the probability that a randomly selected lag time of A after B (B after A) lies in the interval $(t, t+dt)$. We then compute the distance between the distributions of lag times as the Kolmogorov-Smirnov distance [46,47] (D_{KS}) between them, where D_{KS} is defined as the maximum distance between the two cumulative distribution functions P_{AB} and P_{BA} as

$$D_{KS}(P_{AB}, P_{BA}) = \max_t(|P_{AB}(t) - P_{BA}(t)|). \tag{1}$$

We use a signed version of D_{KS} to distinguish which of the two cumulative distributions is greater than the other. Since this quantity is no longer a metric, we refer to it as the Kolmogorov-Smirnov arrow A_{KS} (KS-arrow).

$$A_{KS}(P_{AB}, P_{BA}) = \text{sign}\left(P_{AB}(\tau) - P_{BA}(\tau)\right) D_{KS}(P_{AB}, P_{BA}), \tag{2}$$

where $\tau = \arg\max_t(|P_{AB}(t) - P_{BA}(t)|)$. For measuring the KS-arrow, we find the time, τ, that maximizes the distance between the two compared cumulative distributions, and then draw an arrow from the second to the first distribution (first and second refers to their order in the arguments of the KS-arrow, see Fig 1). If the arrow points upwards, it indicates that the cumulative distribution of the first process is greater than that of the second at the time τ, while if it points downwards, it indicates that the cumulative distribution of the second process is

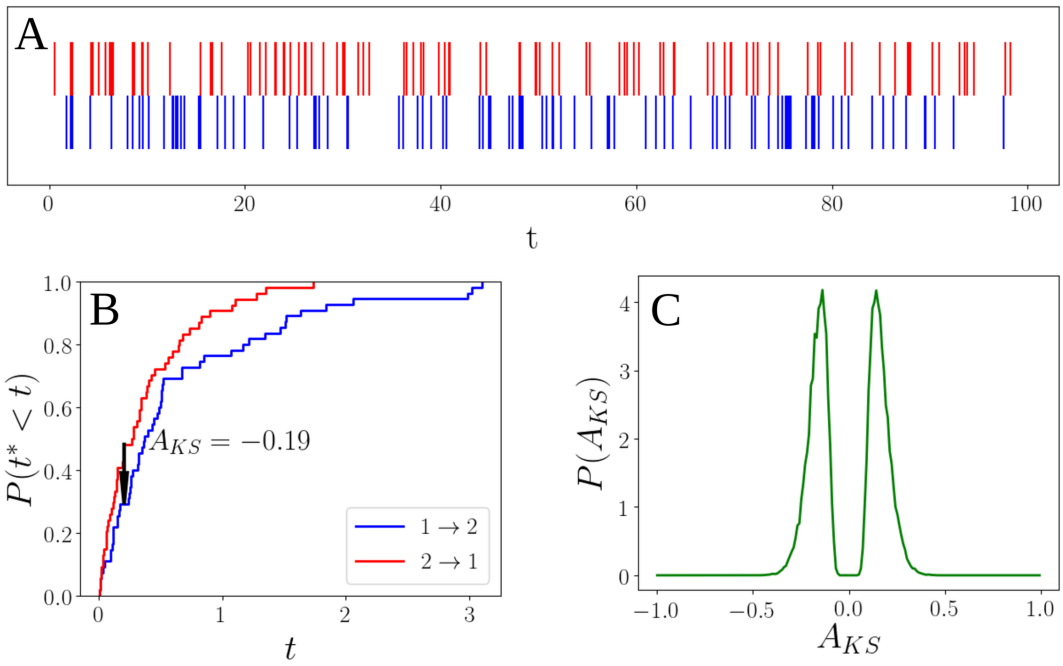

Fig 1. Two independent homogeneous Poisson processes of rate $\lambda = 1$. The sequences were generated up to a maximum time of 100 time units. **A** Raw event data. Individual A in blue and Individual B in red. **B** Cumulative distribution of lag times and KS-arrow, A_{KS}, obtained from the sequences shown above. In blue is the cumulative distribution of lag times of Individual A following Individual B, while in red is its conjugate (lag times of B following A). **C** Distribution of KS-arrows from 10^4 realizations of pairs generated as in the sequences above. The distribution shows two peaks around 0, signature of no leader-follower interaction.

https://doi.org/10.1371/journal.pcsy.0000073.g001

greater than that of the first at τ. The value of the KS-arrow is then given by the maximum distance between the two cumulative distributions multiplied by the sign of their difference at τ. For two interevent sequences $\{t_{AB}\}$ and $\{t_{BA}\}$, $A_{KS}(P_{AB}, P_{BA}) > 0$ implies that times associated with process 1 are shorter than those associated with process 2. Thus, if individual B is following individual A, we will expect $A_{KS}(P_{AB}, P_{BA}) > 0$, while $A_{KS}(P_{AB}, P_{BA}) < 0$ reflects the opposite (A following B). The strength of the interaction will be given by the absolute value of the KS-arrow. The value of the KS-arrow represents the excess probability of observing response times smaller than τ in the cumulative distribution, indicating a stronger leader-follower association where the follower responds more quickly to the leader's dynamics.

We quantify the significance of the KS-arrow by comparing the value calculated from the original acoustic detection dataset to the distribution of KS-arrow values derived through randomised reshuffling and subsequent reanalysis of the detection data. The detection dataset is reshuffled 10^4 times, and the number of detections recorded for each individual are retained, but randomly reassigned. A p-value is then assigned to the measured value of the KS-arrow based on the probability that it is above $|A_{KS}|$ and below $-|A_{KS}|$ in the null distribution.

2.3. Application to synthetic presence data

To test the aforementioned analytical approach, we created synthetic presence data for a pair of individuals (hereafter, individual A and individual B) proposing a model of temporal sequences. The first set of times, corresponding to individual A, is given by a homogeneous

Poisson process of rate λ_A, i.e., individual A appears randomly at a constant rate. The temporal sequence for individual B follows from a non-homogeneous Poisson process with rate $\lambda_B(t)$, which depends on time in such a way that it has a constant rate λ^* plus an excess rate δ in the interval $(-\lambda^*, \infty)$ during an amount of time Δt immediately after the presence of individual A is recorded. Mathematically this can be expressed as

$$\lambda_B(t) = \lambda^* + \delta H\left(\sum_{i=1}^{T}\left[H(t-t_i) - H(t-(t_i+\Delta t))\right]\right), \tag{3}$$

with t_i being the times at which individual A is present, $H(t)$ the Heaviside step function, and T the total number of events of individual A. The parameter δ can be positive or negative, and it represents the excess rate of presence of individual B after the presence of individual A. If $\delta > 0$, then individual B is more likely to be present after individual A, while if $\delta < 0$, then individual B is less likely to be present after individual A. The parameter Δt represents the time window during which this excess rate applies. This is similar to a Hawkes process [48] and to the model for correspondence by Malmgren et al. [49], but in this case the excitations are given by an independent source and are not self-excitations. If $\Delta t = 0$, we have two independent homogeneous Poisson processes of rates λ_A and $\lambda_B(t) = \lambda^*$, whereas for $\Delta t \to \infty$, we have two independent homogeneous Poisson processes of rates λ_A and $\lambda_B = \lambda^* + \delta$. For an intermediate Δt, individual B may attempt to be actively present at, or avoid, the location for a period of time Δt, shortly after individual A was there for a positive, or negative, value of δ, respectively. If $\delta = 0$, we again have two independent Poisson processes of rates λ_A and $\lambda_B = \lambda^*$. In the following, we choose $\lambda_A = 1$ without loss of generality, as we can always rescale time such that one of the rates is unit. From the time series for Individuals A and B we extract the sets of lag times $\{t_{AB}\}$ and $\{t_{BA}\}$ and compute the KS-arrow $A_{KS}(\{t_{AB}\}, \{t_{BA}\})$ so that if $A_{KS} > 0$, individual A is following individual B, and if $A_{KS} < 0$ individual B is following individual A. Several realizations of the process are simulated, and the distribution of KS-arrows compiled to examine whether the KS-arrow is able to capture the aforementioned leader-follower behaviors (see Figs 1 and 2).

For two independent Poisson processes of different rates ($\delta = 0, \lambda_A \neq \lambda_B$), the distribution of KS-arrows are always symmetric, with low values centered around, but not equal to, zero (see Fig 1). This reflects the fact that the sequences are uncorrelated, and that it is not possible to discern if one individual is following the other. The absence of values around zero is related to the fact that the KS-arrow will only be zero if the compared distributions are exactly equal. This equality will be only occur when the sampling is infinite, which was confirmed by drawing longer and longer time series sequences and observing that the distribution collapsed towards a single delta function at zero (not shown here). Regarding the correlated case, *i.e.* when $\delta \neq 0$, we examined how the distribution of KS-arrows changes as we change the parameters δ and Δt, setting $\lambda^* = 1$ (not shown here). If $\delta = 0, \Delta t = 0$ or Δt much bigger than $1/\lambda_A$ the distribution is symmetric around 0 with values close to it, reflecting again that there is no evidence of one individual following the other, as expected for independent presence sequences. For $\delta < 0$, the distribution is non-zero only for positive values of the KS-arrow, indicating that the first individual follows the second (although the model is just assuming that the second one is avoiding the first one), while for $\delta > 0$ the distribution is shifted to negative values of the KS-arrow, showing that the second individual is following the first (like shown in Fig 2). To accurately differentiate between leader-follower behavior and avoidance behavior, it is crucial to analyze the appearance probabilities of individuals following one

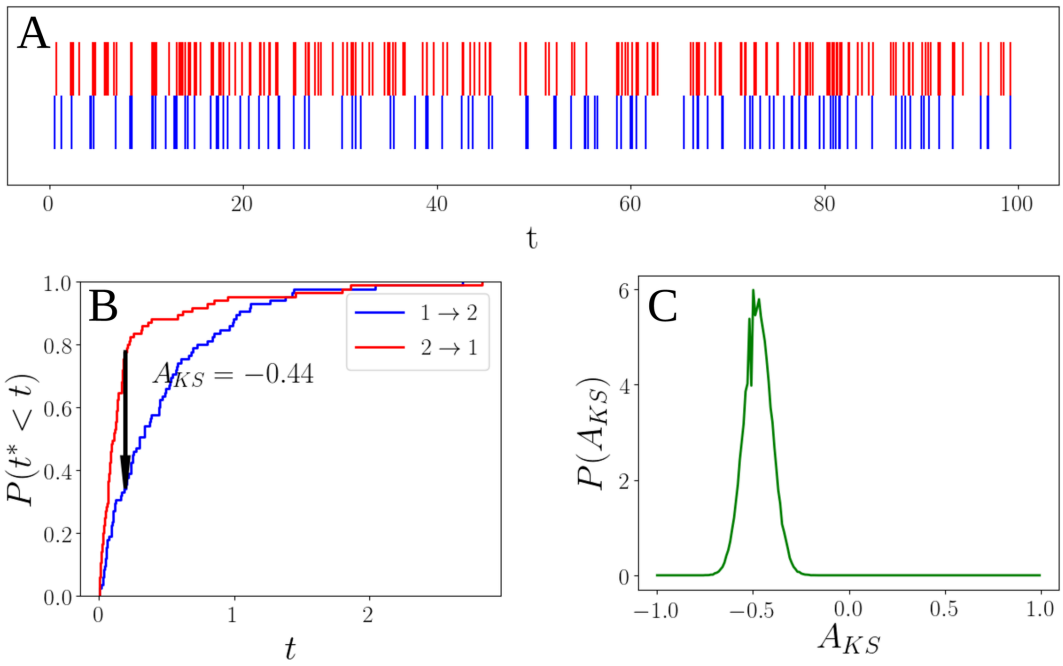

Fig 2. Correlated time sequences. Individual A (blue) performs a homogeneous Poisson process of rate $\lambda_A = 1$, while Individual B (red) follows the correlated non-homogeneous Poisson process described in the text with parameters $\lambda^* = 1, \Delta t = 0.2$ and $\delta = 4$, i.e., it performs a Poisson process of rate $\lambda_B = 1$ except for 0.2 units of time after an event of Individual A, when it performs a Poisson process of rate $\lambda_B = 5$. The sequences were generated up to a maximum time of 100 time units. **A** Raw event data. **B** Cumulative distribution of lag times and KS-arrow for the sequences shown above. **C** Distribution of KS-arrows from 10^4 realizations of pairs generated as in the sequences above.

https://doi.org/10.1371/journal.pcsy.0000073.g002

another. While both behaviors may yield similar distributions of KS-arrows, their underlying dynamics are fundamentally different. In a leader-follower scenario, we expect a consistent pattern where one individual tends to appear after the other, indicating a directional influence. Conversely, in an avoidance scenario, the relationship may appear random or independent, with individuals avoiding each other rather than following. To discern these behaviors, we propose a detailed examination of the appearance rates of one individual after the other. By comparing these probabilities, we can identify patterns that suggest either a leader-follower or an avoidance interaction. In particular, we performed the following test: we computed the appearance rates of one individual after the other and vice versa, both for lag times t shorter and longer than the characteristic time τ. This analysis provides deeper insights into the interactions between the individuals and helps clarify the nature of their relationship in the observed data.

Lastly, we examined the behavior of the distribution of KS-arrows when the two time series sequences were reshuffled in such a way that both individuals retained the same number of events, but without correlations, if there were any. For both the correlated and uncorrelated cases, the result was the same: the distribution of KS-arrows for the reshuffled sequences is typical of a pair with no leader-follower interactions, i.e., with low KS-arrow values, centered around but not equal to zero (see Fig 3). Actually if the pair of sequences corresponds to two independent random sequences, the distribution of KS-arrows for the reshufflings is identical to the distribution of KS-arrows for the original ensemble of sequences (Fig 3A); while for the case of correlated sequences both distributions differ (Fig 3B). This result allows the discernment of whether a KS-arrow value, A_{KS}, is significant, as one can compute the p-value of the

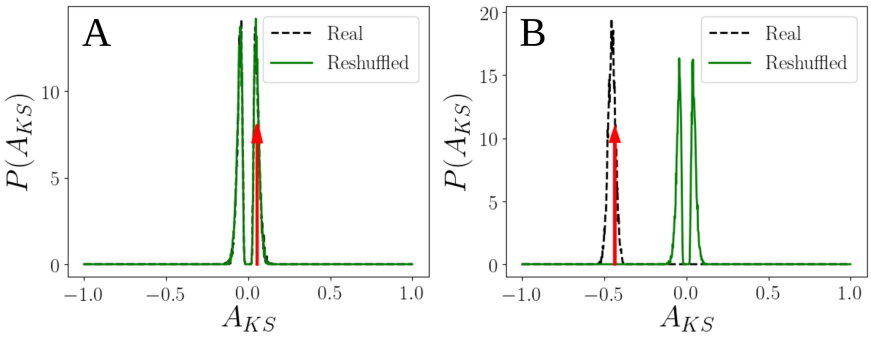

Fig 3. Assessing significance of the leader-follower interactions. A Random uncorrelated sequences with $\lambda_A = \lambda_B = 1$ and $t_{\max} = 10^3$. In dashed black lines the distribution of KS-arrows for the ensemble of those sequences (10^4 independent realizations). In green is the distribution of KS-arrows for 10^4 reshufflings of the pair of sequences that gives rise to the KS-arrow value marked in red. **B** Correlated sequences with $\Delta t = 0.2$, $\delta = 4$ and a maximum time of 10^3 time units. The KS-arrow distribution for these ensemble of sequences is shown in black (10^4 independent realizations), while in green is the distribution of KS-arrows coming from 10^4 reshufflings of the sequence pair that gives rise originally to the value of the KS-arrow signaled at the red line.

https://doi.org/10.1371/journal.pcsy.0000073.g003

KS-arrow found for the real pair of sequences by calculating the amount of probability that is above $|A_{KS}|$ and below $-|A_{KS}|$ in the distribution of KS-arrows coming from the reshufflings. This is the probability that a value higher than $|A_{KS}|$ or lower than $-|A_{KS}|$ comes from a pair of random sequences.

2.4. A case study: Reef manta rays (*Mobula alfredi*) at a cleaning station

We apply the described leader-follower analysis methodology to presence data collected for acoustically-tagged reef manta rays (*Mobula alfredi*) at a frequently visited site, known as a cleaning station, at a remote coral reef in Seychelles. The resulting social network and reported leader-follower interactions are then examined relative to the sex and size of tagged manta rays.

2.4.1. Data collection. Presence data for reef manta rays were collected using passive acoustic telemetry, whereby a single acoustic receiver (VR2W; VEMCO) was placed in close proximity to a known cleaning station at D'Arros Island, Seychelles [21]. Twenty-five acoustic tags (n = 4, V12; n = 21, V16-5H) were externally deployed on free-swimming reef manta rays using a modified Hawaiian sling between April 2013 and March 2014. Tag anchors were made of either titanium (n = 4) or stainless steel (n = 21), and were positioned towards the posterior dorsal surface of each individual. Prior to tag deployment, a photograph was taken of the unique and consistent spot pattern present on the ventral surface of each manta ray [43,50] to allow for individuals to be identified in future monitoring surveys. The sex of each individual was determined by the presence (male) or absence (female) of claspers, and size (i.e. wingspan) was visually estimated to the nearest 0.1 m. Individuals were classified into one of the following two size groups based on their estimated size: small (1 female, 9 males), and big (9 females, 6 males). The small class included juvenile (any individual $\leq$2.4 m) and sub-adult individuals (male: 2.5–2.8 m; female: 2.5–3.1 m), while the big class included only adult individuals (male: $\geq$2.9 m; female: $\geq$3.2 m) as per [51,52].

Detection data from the cleaning station receiver were downloaded every six months, and once a year the battery was replaced and the receiver inspected for damage or clock drift. Preliminary range testing indicated a detection radius of approximately 150m (mean = (165 ± 33)m [27]) at the cleaning station receiver. Upon import of the detection data into a

Microsoft Access database, false positive detections were removed through filtration for active tags and any receiver clock-drift time corrections were calculated assuming linear drift [27]. In total, 41,607 detection events were recorded between April 2013 and January 2016. The temporal accuracy of the detection timestamps is in seconds.

2.4.2. Measuring temporal heterogeneities. We measure the hourly appearance probability of each individual in order to investigate the circadian patterns of residence in the vicinity of the study site, as the percentage of events recorded during each hour of the day. We also compute the distribution of times between consecutive events of the same individual, called interevent times. In many natural phenomena, including human activities or earthquake events these interevent time distributions follow fat-tailed distributions with a power law tail. The exponent of the tail has been fitted using the 'powerlaw' package available for python [53].

2.4.3. Leader-follower network. To construct the leader-follower network, we analyze the interactions occurring between pairs of tagged manta rays. Interactions are defined as the presence of one individual and a consecutive appearance of the other. For statistical purposes, we considered only the pairs with more than 50 interactions ($n = 12$ individuals). We then assess the value and direction of the KS-arrows between the distribution of lag times for each pair, as described above. We use a global reshuffling scheme to compute the p value associated with each KS-arrow, and discard those for which $p > 0.025$. This cutoff balances the trade-off between Type I errors (false positives) and Type II errors (false negatives). This threshold is commonly used in exploratory studies to ensure that significant measures are identified while maintaining a controlled rate of false positives. After applying the Bonferroni correction to account for multiple comparisons (given that each time series is compared with 11 others), the corrected p-value threshold becomes 0.0023. This choice reflects a compromise between statistical rigor and the ability to detect meaningful patterns in the data, ensuring that the identified interactions are both statistically significant and biologically relevant. The reshuffling scheme allows for the number of detections for each individual to remain fixed, but for the timing of the events to be reshuffled from the pool of all detections. This differs from a local reshuffling scheme, which was also trialed and where only the two sequences involved in the calculation of the KS-arrow are involved in the reshuffling, however, both schemes lead to similar results.

In order to assess the correlation of sex and individual size with the topology of the network, we compare two basic quantities: (1) the number of edges present in the network of each type and (2) the average weight of the edges. Comparisons were drawn across 10^4 reshufflings of the sexes and sizes, respectively, but keeping the network structure fixed, *i.e* we kept the number of individuals of each type (male or female and big or small) and distribute the labels randomly to the individuals. We do not keep the pairs sex-size due to the reduced number of individuals, breaking thus their correlation. These ensembles of networks with reshuffled sex and sizes are used as a null model and set the expected values for the number of edges and their average weight. The null model is used to assess whether the observed network structure deviates significantly from what would be expected by chance, given the fixed number of individuals of each type. This approach allows us to determine if the observed patterns in the leader-follower network are statistically significant or simply a result of random variation in the data.

We also observe that the inferred interactions follow from a leader-follower behavior. For each pair of individuals where a KS-arrow points from individual A to individual A, we compute the probability of A appearing as a function of time since the last appearance of B. This probability is expected to decay over time. When reversing the measure to calculate the appearance probability of individual B after A, the resulting curve should lie below the

original to signal leader-follower interactions. This is further evaluated for every inferred interaction by comparing the appearance rates of both individuals for lag times shorter and longer than the characteristic time τ associated with the maximum difference in their cumulative distributions. The pattern shown by the artificial presence model for leader-follower and avoidance behavior is then compared to the observed data to confirm the nature of the interaction.

3. Results: Manta rays case study

A total of 41,607 detections of acoustically-tagged reef manta rays (1 small female, 9 small males, 9 big females and 6 big males) were recorded at the cleaning station receiver between April 2013 and January 2016.

The manta detection data are not distributed evenly in time, but rather in a highly inhomogeneous way. In Fig 4A we show the distribution of events for mantas with more than 100 detections (n = 18 individuals). Detections are most commonly recorded around noon, with an evident circadian pattern (Fig 4B). Interevent times are distributed following a heavy-tailed distribution, with a tail consistent with a power law of exponent 1.38 (Fig 4C). This implies that the temporal appearances of the manta rays at the cleaning station are burst-like, with periods of high activity followed by long times of inactivity and individual absences. The distribution also shows a peak located at a time of one day, which is a reflection of the circadian pattern (i.e. 24 hr) of the manta rays.

The final network constructed for reef manta rays at the cleaning station consists of 12 individuals; five females (one small, four big) and seven males (three small and four big). A total of 33 edges, representative of calculated KS-arrows, are included in the network to generate a single component (Fig 5A). Regarding the sexes, and when comparing to the null model of reshuffled sexes, mixed edges (male following female or female following male) are on average stronger than expected, much more so for males following females, although there are many fewer males following females than expected, in contrast to females following males, which are overrepresented. For same sex edges, the results reflect a randomized scenario. That is, while the number of edges present is as expected, their strength is smaller than expected (see Fig 5B). As for the sizes, and when comparing to the null model of reshuffled sizes, the most salient result is that the average weight of the interactions of small individuals following small individuals is much lower than expected. The other types of edges are only slightly off the values that are expected. So, small individuals following big individuals do so at a stronger frequency than expected and there is one link less than expected. For big reef manta rays following small ones, the strength is slightly weaker than expected and there is only one extra edge. For big individuals following other big conspecifics, the strength of the interaction is slightly higher than expected, and there are only two more edges than expected (see Fig 5C).

In Fig 6 we show the average appearance rate averaged over all pairs. The appearance rate is computed for one individual as a function of the time since the last presence event of the other individual, but restricting to pairs for which there is a connection in the inferred network. One can see that the appearance rate for followers is bigger than for leaders up to a certain time lag of around 200 minutes. This enhanced appearance rate of the following individuals after the appearance of the individual that they follow is compatible with our measurement of leader-follower behaviors.

Using the presence model, we find that for avoidance behavior, the individual exhibiting avoidance shows a lower appearance rate for lag times shorter than τ compared to the other, while for lag times longer than τ both rates become similar. In contrast, for leader-follower behavior, both appearance rates are similar for lag times shorter than τ, but for lag times

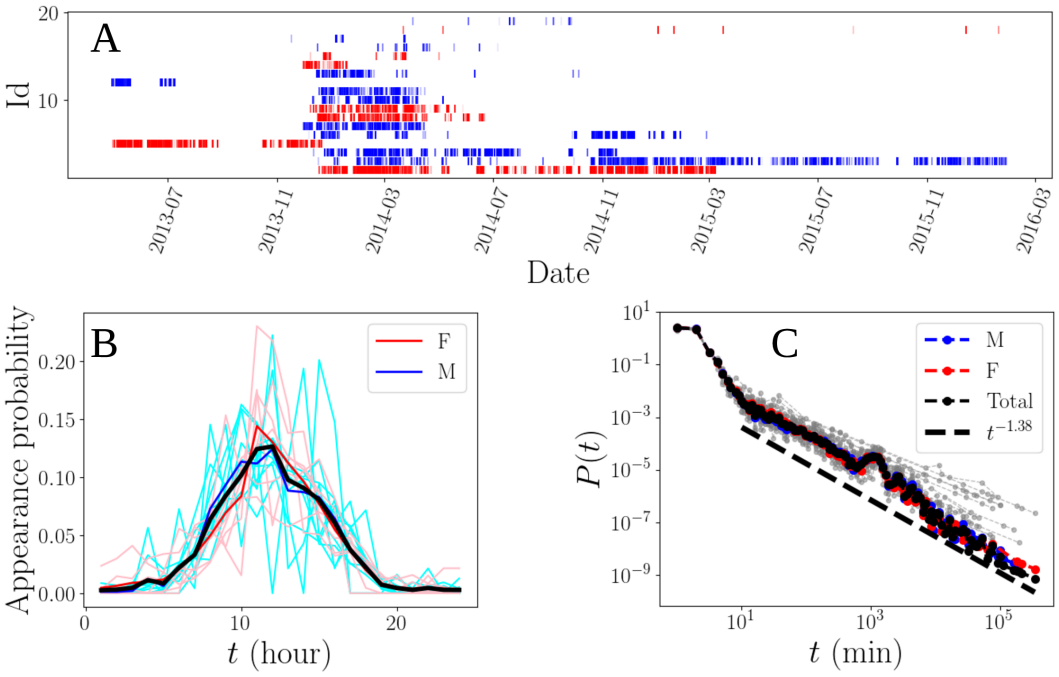

Fig 4. Temporal heterogeneities in the data. A Raw event data for acoustically-tagged reef manta rays (*Mobula alfredi*) with more than 100 detection events (females in red and males in blue). The heavy-tailed inter-event time distribution (see **C**) causes detections to cluster into brief bursts flanked by long gaps. In the figure we see these bursts as compact horizontal bands where numerous second-precision detections merge into single streaks. **B** Appearance probability as a function of the hour in the day. The cyan lines correspond to different males, while the pink lines correspond to different females. The red and blue lines are the averages for females and males respectively. The black curve corresponds to the appearance probability of all individuals pooled. **C** Interevent times distribution, i.e., the distribution of times between consecutive presence events of the same individual.

https://doi.org/10.1371/journal.pcsy.0000073.g004

longer than τ the following individual exhibits a higher appearance rate (see supplementary S1 Fig). When applying this test to the real data, we find that for the edges with sufficient data to perform the analysis (5 out of 51), the observed pattern consistently matched that of following behavior. This indicates that, to the extent that our data allow, the inferred interactions are of the leader-follower type rather than avoidance.

4. Discussion

Leadership analyses represent a source of behavioral information. For example, the presence or absence of leadership between adult and juvenile individuals provides insight into the learning strategies of a species, which can be biased towards learning from adults (i.e., juveniles following them), or towards learning through trial and error (i.e., displaying independent behavior) [8]. Additionally, leadership analyses can be used to reveal long-term hierarchies in animal groups and aid in characterizing the structure of populations [10].

Here we made use of delays in the appearance of individuals at a location to infer leader-follower interactions. Delays, which are already known to modulate ecological dynamics in different ways [54], have thus proven to be a useful proxy for the directionality of interactions, and can be used to construct directed networks from presence data. We introduced a statistical method for the inference of leadership patterns recorded in presence data collected at a single location. At the base of the method is the comparison of lag-time distributions with a

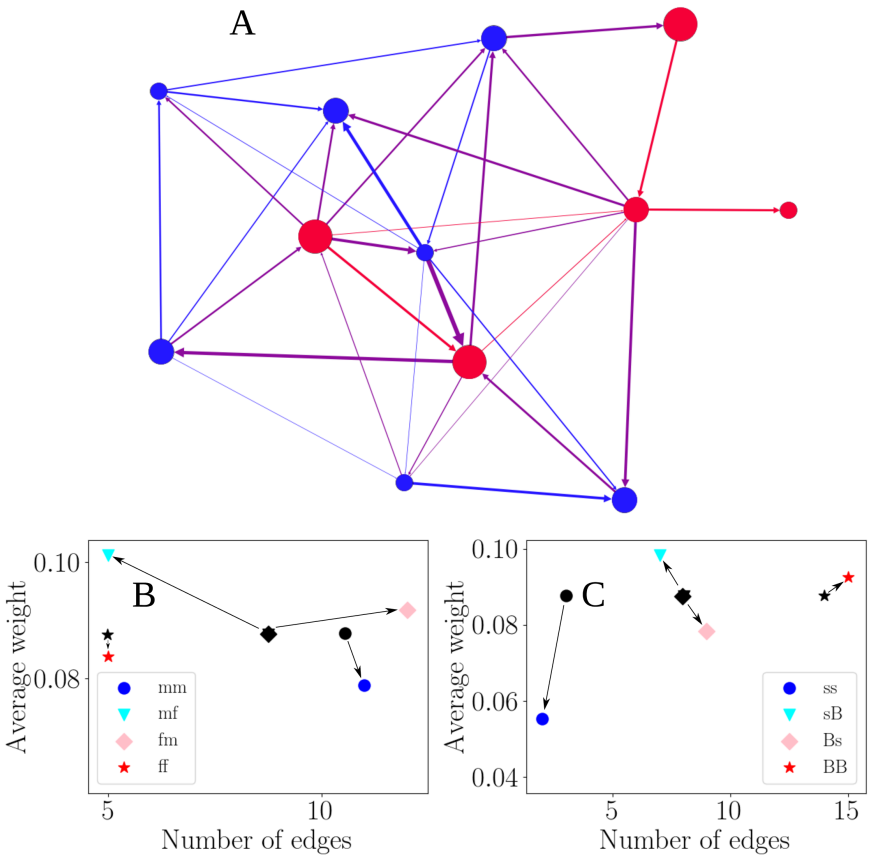

Fig 5. Leadership network for acoustically-tagged reef manta rays (*Mobula alfredi*) detected by a single acoustic receiver placed at a cleaning station at a remote coral reef in Seychelles relative to the sex (Female, pink; Male, blue) and size (node size) of individuals. A Leader-follower network of manta rays at a confidence value $p = 0.0023$. The nodes have been positioned using a force-directed algorithm and then repositioned manually for clarity of the visualization. **B** and **C** Types of edges depending on sex and size. An edge of type xy stands for an individual of type x following an individual of type y, where x and y can be f (female) or m (male) for the sexes, or s (small) and B (big) for the sizes. The black symbols are the expected values from 10^4 reshuffling of the sexes/sizes of the individuals. The x-axis shows the number of such edges, while the y-axis shows the average strength of the edges. Deviation of the real data in the x direction indicates a difference of the number of edges of that kind found in the real network. Deviation in the y direction signals a difference with the expected strength of the leader-follower interactions. The arrows show how the results from the original network differ from the results of randomizations.Results for the randomization of sexes.

https://doi.org/10.1371/journal.pcsy.0000073.g005

variation of the Kolmogorov-Smirnov distance. Although other distance or similarity measures can be used in the same way, we used this one for three main reasons: it is sensitive to the shape of the distributions, it is non-parametric and does not assume specific distributions, and it is robust to outliers. The method relies on randomizations of the input data, which provide estimates for the p-values associated with the leader-follower interactions found. We have tested this methodology against intuitive models of leading behavior, and applied it to a real-world scenario involving presence data for reef manta rays at a cleaning station recorded using passive acoustic telemetry. Our method allowed us to construct a directed network from the manta detection data, which represents leader-follower interactions within the tagged population, and examine whether covariates such as sex and size affect the position of the individuals in the network. Female manta rays were found to follow more males than expected,

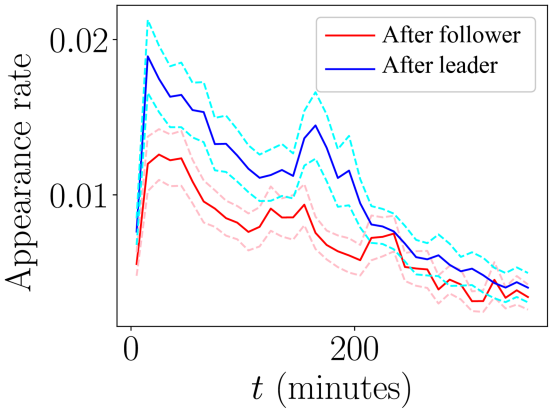

Fig 6. Appearance rate for the follower right after the appearance of the leader (blue) or for the leader after the appearance of the follower (red). The rates show that the follower actually has a higher rate of appearing right after an event of the leader. The curves show the average for all the pairs present in the network. The dashed lines show the standard errors.

https://doi.org/10.1371/journal.pcsy.0000073.g006

while males followed fewer females, but with a stronger association. With respect to size, smaller mantas followed other small mantas with a weaker interaction strength, whereas the remaining interactions within the network exhibited a pattern similar to that expected from the randomized case. Furthermore, we examined whether there is an enhanced probability of the appearance of a follower after the appearance of a leader at the cleaning station, and confirmed that the associations found within the study are of a leader-follower nature.

The leader-follower network inferred in this study represents directional interactions between individuals, based on the likelihood that one individual appears after another at the monitored site. Each directed edge in the network indicates a statistically significant tendency for the follower to be detected after the leader, as determined by the KS-arrow and its associated p-value. While there is no absolute benchmark for leader-follower interactions in this context, the reshuffling approach provides a relative measure of significance, allowing us to identify interactions that are unlikely to arise by chance alone.

The main achievement and uniqueness of our approach is the use of the KS distance to compare lag-time distributions, which captures both the central tendency and the shape of the temporal relationships between individuals. This method, combined with a robust statistical framework based on data reshuffling, enables the inference of directional (leader-follower) interactions from presence data alone. Our approach is generalizable and can be applied to other systems where only temporal interaction data are available, offering a new avenue for studying social dynamics in animal populations and beyond.

Comparison with other similar works. Ref [34] examines the associations among reef manta rays based on sighting data recorded using photo-identification techniques at five locations in Indonesia for five years. This presents a unique opportunity to compare sampling, network analysis techniques, and findings between two populations of reef manta rays. While the photo-identification data set of Ref [34] spans a longer temporal range than that of the present study, data collection was restricted to daylight hours only. In contrast, the automated data collection facilitated by the acoustic receivers and tags of this study allowed for presence data to be collected across the entire diel cycle. This allowed for a more detailed and dynamic approach to the examination of leader-follower interactions in reef manta rays to be developed, and made it possible to move beyond traditional associations defined using the

"Gambit of the Group" (i.e. assuming that all individuals observed together are associated). Note that this difference is crucial, since in our framework, two individuals, even if observed always together, might not be related by a leader-follower interaction depending on the timing of the presence events.

Nevertheless, it is interesting to compare results between populations and datasets in terms of the influence of sex and size on network position. Perryman et al. found that male reef manta rays tend not to associate with other males, and for them avoidance is common, whereas females may be associated significantly with other females. The highest percentage of preferred dyadic associations was given between different sex pairs, however, there was partial sexual segregation. Regarding maturity status, Perryman et al. found that juveniles tend to associate in the short term with other juveniles and mature adults. It is challenging to determine whether the differences in findings between this, and the present study, are the result of natural behavioral differences or are artifacts of differing analysis procedures. Should acoustic data become available for reef manta rays at any of the five Indonesian field sites used by Perryman et al., future works should aim to replicate the leader-follower analyses outlined here and to compare the results with the findings of the photo-identification-based study.

Ref [32] describes a method for extracting social structure information from data similar to that of the present study, but again, relies on the Gambit of the Group theory. The major drawback of this method (available within the package GMMevents) is that it relies on clustering the observations of associations into different event windows, as observations occur in bursts. In many situations, these events windows may be very difficult to define, as the inter-event times of the observations appear power-law distributed, without a clear cut for the clusters, and it may be that association data is lost in the process. Ref [14] builds upon the methodology described in Ref [32], and allows 'leadership' behavior to be inferred. This is achieved by investigating which animal appears first in the association events that the clustering method has identified, however, by doing so, eliminates all of the information about the dynamics contained in the timings of observations inside the event. Our method does not separate times into classes (such as being part of an event), and instead, considers the complete temporal range of the data, making the analysis procedure less prone to ambiguities and information loss while allowing for leadership behaviors to be examined.

Limitations and future work. A key limitation of our approach arises from the spatial and temporal resolution of the acoustic telemetry data. Detections are registered when tagged individuals are within approximately 150 m of the receiver, meaning that two individuals detected at nearly the same time could, in reality, be separated by up to 300 m. This spatial uncertainty implies that some inferred interactions may not correspond to direct social encounters, but rather to coincident presence within the detection range. However, we expect that such spurious co-detections would generate balanced waiting times, similar to those produced by random appearances, and thus would not systematically bias the inference of directed interactions.

Nevertheless, we acknowledge that our method cannot fully disentangle leader-follower behavior from correlated presence patterns that may arise due to shared environmental preferences, foraging behavior, or physiological differences among individuals. While the observed asymmetries in appearance rates and lag-time distributions are consistent with leader-follower behavior, alternative explanations such as environmental drivers or avoidance cannot be entirely excluded. Due to data limitations, we were able to apply our appearance rate test to only 5 out of the 51 edges (approximately 10% of the network), as the remaining edges did not have sufficient data to perform the analysis reliably. Importantly, in all cases where the test was feasible, the observed patterns were consistent with leader-follower behavior rather than avoidance. Therefore, while our results provide support for the inference of

leader-follower interactions, this evidence should be interpreted with caution, and future studies incorporating higher spatial resolution or additional behavioral observations would be valuable to further validate these findings.

The analytical method proposed in this study allows only for the detection of paired (i.e. dyadic) interactions from presence data collected at a single location, however, cannot currently be used to detect more complex, collective behaviors. Expanding these analysis to encompass data collected by multiple acoustic receivers placed at different locations (i.e. acoustic arrays; e.g [21]) will allow for leadership networks to be described using a multilayer approach [55], whereby each receiver is considered as a different layer. Such an approach may reveal if leadership patterns are coherent among different locations that may be significant for different ecological reasons (e.g. cleaning, feeding), if followers continue to follow their leader across wider spatial scales, or if interactions are more complex and followers in one location become leaders in another. Another possible application of our methodology would be to use it in the study of biomimetic systems [56]. For now, however, the present methodology can be applied to existing acoustic telemetry data sets around the globe, and may reveal previously unidentified leader-follower behaviors and patterns in marine species across various ecosystem types. The application of acoustic telemetry and leader-follower network analysis provides valuable insights for conservation and management of reef manta rays and their habitats. By identifying key individuals, social structures, and patterns of site use, managers can better understand how and when interaction may be occurring within an area. By monitoring changes in social network structure or site fidelity over time, it may be possible to detect early signs of ecological stress or anthropogenic impact, such as habitat degradation or increased human presence. Quantified changes in network connectivity, visitation rates, or shifts in leader-follower behavior may serve as indicators of risk, helping to guide adaptive management strategies aimed at reducing ecological stress and supporting the long-term viability of both the species and their habitats.

A promising avenue for future research is the integration of non-linear modeling approaches, such as Convergent Cross Mapping (CCM) [57], to better capture the complex, non-linear interactions underlying leader-follower behavior in manta rays and other ecological systems. Unlike simple correlation-based methods, CCM and related techniques can help infer causality and account for dynamical heterogeneity, divergence, and asynchronicity in animal encounters [58,59]. Additionally, extending the analysis to include spatially explicit environmental variables (e.g., water currents, temperature, or habitat quality) and eco-environmental network frameworks [60] would allow for a more comprehensive understanding of how environmental factors shape social interactions and collective movement. Analyzing the temporal evolution of the leader-follower network, and quantifying departures from ideal network configurations, could provide early-warning indicators of ecological stress or regime shifts [59].

Another important direction is the application of global sensitivity and uncertainty analysis (GSUA) to the leader-follower network and associated ecological variables [61]. GSUA methods, including variance-based and entropy-based approaches, can identify the key determinants of model and data variability, as well as high-order interactions among variables that may drive observed patterns. By systematically attributing uncertainty, it becomes possible to quantify ecological stress and disentangle the contributions of environmental drivers, biological factors, and unknown sources of variability. Such analyses would enhance the robustness and interpretability of network-based ecological indicators, and could be facilitated by existing GSUA toolkits (e.g., SAFE toolbox).

Finally, future work should focus on assessing the stability and resilience of ecological networks over space and time, and under varying environmental conditions. By tracking how

network indicators (e.g., connectivity, centrality, or modularity) change in response to environmental gradients or perturbations, it is possible to identify stable states, critical transitions, and optimal network configurations for ecological functioning [59]. Monte Carlo filtering and other probabilistic approaches can be used to explore the probability distributions of network metrics and their sensitivity to different predictors, providing a basis for mapping site- or time-specific patterns and for developing adaptive management strategies. Such systemic analyses will be essential for understanding and managing the complex interplay between ecological processes and environmental change.

Supporting information

S1 Fig. Differentiating leader-follower and avoidance interactions. A The method detects a relationship with a KS-arrow from individual B to individual A, which could represent a leader-follower (A as leader, B as follower) or an avoidance (A avoiding B) interaction. **B** and **C** show the average appearance rates of A after B (green) and B after A (purple) for lag times t shorter and longer than the characteristic time τ identified by the method. For leader-follower dynamics (**B**), the rates are similar for short lag times ($t < \tau$), but for long lag times ($t > \tau$), the leader's appearance rate decreases while the follower's rate remains consistent. Results are based on the artificial presence data model with $\delta = 2$, $\Delta t = 1$, time series length of 2000, and 500 realizations. For avoidance dynamics (**C**), the avoider's appearance rate is lower than the avoided individual's for short lag times ($t < \tau$), while both rates become similar for long lag times ($t > \tau$). These results use the artificial presence data model with $\delta = -0.95$, $\Delta t = 1$, time series length of 2000, and 500 realizations.
(TIFF)

Acknowledgments

VME and JFG acknowledge partial support from projects MISLAND (PID2020-114324GB-C22) and CSxAI (PID2024-157526NB-I00) funded by MICIU/AEI/10.13039/501100011033/ FEDER, UE. JPR was supported by Govern de les Illes Balears through the Vicenç Mut program. Fieldwork and data collection was funded by the Save Our Seas Foundation (SOSF) and supported by The Manta Trust and SOSF – D'Arros Research Centre (SOSF-DRC). Collection of acoustic telemetry data in Seychelles was approved by, and conducted with the knowledge of, the Seychelles Bureau of Standards and the Seychelles Ministry of Environment, Energy and Climate Change.

Author contributions

Conceptualization: Juan Fernández-Gracia, Jorge P. Rodríguez, Víctor M. Eguíluz.

Data curation: Lauren R. Peel.

Formal analysis: Juan Fernández-Gracia, Jorge P. Rodríguez, Konstantin Klemm, Víctor M. Eguíluz.

Methodology: Juan Fernández-Gracia, Jorge P. Rodríguez, Konstantin Klemm, Víctor M. Eguíluz.

Resources: Mark G. Meekan.

Software: Juan Fernández-Gracia.

Writing – original draft: Juan Fernández-Gracia.

Writing – review & editing: Juan Fernández-Gracia, Jorge P. Rodríguez, Lauren R. Peel, Konstantin Klemm, Mark G. Meekan, Víctor M. Eguíluz.

References

1. Ren J, Sun W, Manocha D, Li A, Jin X. Phy Rev E. 2018;98(5):1–8.
2. Gernat T, Rao VD, Middendorf M, Dankowicz H, Goldenfeld N, Robinson GE. Proceedings of the national academy of sciences of the United States of America. 2018;115(7):1433–8.
3. Chen S, White BJ, Sanderson MW, Amrine DE, Ilany A, Lanzas C. Scientific reports. 2014;4:1–7.
4. Couzin ID, Krause J, James R, Ruxton GD, Franks NR. J Theor Biol. 2002;218(1):1–11.
5. Couzin ID, Krause J. Adv Study Behav. 2003;32:1–75.
6. Sumpter DJ. Philosophical transactions of the royal society B: biological sciences. Phil Transac Royal Soc B: Biol Sci. 2006;361(1465):5–22.
7. Ballerini M, Cabibbo N, Candelier R, Cavagna A, Cisbani E, Giardina I, et al. Proceed Nat Acad Sci United States of America. 2008;105(4):1232–7.
8. Galef BG, Laland KN. BioSci. 2005;55(6):489.
9. Ward AJW, Herbert-Read JE, Sumpter DJT, Krause J. Proc Natl Acad Sci USA. 2011;108:2312–5.
10. Sih A, Hanser SF, McHugh KA. Behavioral Ecology and Sociobiology. Behav Ecol Sociobiol. 2009;63(7):975–88.
11. Krause J, James R, Croft DP. Philosoph Transac Royal Soc B: Biol Sci. 2010;365(1560):4099–106.
12. Ohtsuki H, Hauert C, Lieberman E, Nowak MA. Nature. 2006;441(7092):502–5.
13. Newman M. Networks: an introduction. OUP Oxford; 2010.
14. Jacoby DM, Freeman R. Trends in ecology and evolution. Trends Ecol Evol. 2016;31(4):301–14.
15. Krause J, Lusseau D, James R. Behavioral ecology and sociobiology. Behav Ecol Sociobiol. 2009;63(7):967–73.
16. Blondel VD, Decuyper A, Krings G. EPJ Data Sci. 2015;4(1):1–55.
17. Krause J, Krause S, Arlinghaus R, Psorakis I, Roberts S, Rutz C. Trend Ecol Evol. 2013;28(9):541–51.
18. Germanov ES, Marshall AD. PLoS ONE. 2014;9(10):1–9.
19. Albanese B, Angermeier PL, Gowan C. Transac Am Fish Soc. 2003;132(5):925–39.
20. Cameron LW, Roche W, Green P, Houghton JD, Mensink PJ. Fisheries Res. 2018;207(June):25–7.
21. Peel L, Stevens G, Daly R, Keating Daly C, Lea J, Clarke C, et al. Mar Ecol Prog Ser. 2019;621:169–84.
22. McAuley RB, Bruce BD, Keay IS, Mountford S, Pinnell T, Whoriskey FG. Marine and Freshwater Res. 2017;68(8):1518–31.
23. Carrier JC, Simpfendorfer CA. Shark research: emerging technologies and applications for the field and laboratory. CRC Press, Taylor & Francis Group; 2018.
24. Steckenreuter A, Hoenner X, Huveneers C, Simpfendorfer C, Buscot MJ, Tattersall K, et al. Marine Freshwater Res. 2017;68(8):1403–13.
25. Crossin GT, Heupel MR, Holbrook CM, Hussey NE, Lowerre-Barbieri SK, Nguyen VM, et al. Ecol Appl. 2017;27(4):1031–49.
26. Stewart JD, Jaine FR, Armstrong AJ, Armstrong AO, Bennett MB, Burgess KB, et al. Frontiers in marine science. Front Marine Sci. 2018;5(SEP):1–27.
27. Lea JS, Humphries NE, von Brandis RG, Clarke CR, Sims DW. Proceed Royal Soc B: Biol Sci. 2016;283(1834).
28. King AJ, Johnson DD, Van Vugt M. Curr Biol. 2009;19(19):R911–6.
29. Flack A, Nagy M, Fiedler W, Couzin ID, Wikelski M. Science. 2018;360(6391):911–4.
30. Garland J, Berdahl AM, Sun J, Bollt EM. Chaos. Chaos. 2018;28(7).
31. Corominas-Murtra B, Goñi J, Solé RV, Rodríguez-Caso C. Proceed Nat Acad Sci United States of America. 2013;110(33):13316–21.
32. Psorakis I, Roberts SJ, Rezek I, Sheldon BC. J Royal Soc Interface. 2012;9(76):3055–66.
33. Psorakis I, Voelkl B, Garroway CJ, Radersma R, Aplin LM, Crates RA, et al. Behav Ecol Sociobiol. 2015;69(5):857–66.
34. Perryman RJ, Venables SK, Tapilatu RF, Marshall AD, Brown C, Franks DW. Behav Ecol Sociobiol. 2019;73(8).
35. Lauw HW, Lim EP, Pang H, Tan TT. Comp Math Org Theory. 2005;11(2):97–118.

36. Whitehead H. Analyzing animal societies: quantitative methods for vertebrate social analysis. University of Chicago Press; 2008.
37. Oh KP, Badyaev AV. Am Naturalist. 2010;176(3).
38. Gero S, Engelhaupt D, Rendell L, Whitehead H. Behav Ecol. 2009;20(4):838–43.
39. Krings G, Karsai M, Bernhardsson S, Blondel VD, Saramäki J. EPJ Data Sci. 2012;1(1):1–16.
40. Aplin LM, Farine DR, Morand-Ferron J, Cole EF, Cockburn A, Sheldon BC. Ecol Lett. 2013;16(11):1365–72.
41. Brent LJ, Heilbronner SR, Horvath JE, Gonzalez-Martinez J, Ruiz-Lambides A, Robinson AG, et al. Scient Rep. 2013;3:1–8.
42. Stevens GM, Hawkins JP, Roberts CM. J Fish Biol. 2018;93(2):344–59.
43. Marshall AD, Dudgeon CL, Bennett MB. Marine Biol. 2011;158(5):1111–24.
44. Stevens GMW. Conservation and population ecology of manta rays in the Maldives. University of York; 2016.
45. Fernández-Gracia J. 2020. https://github.com/juanfernandezgracia/leadership_package.
46. Kolmogorov AN, Shiryaev AN. Selected works II: probability theory and mathematical statistics. Springer Netherlands; 2012.
47. Statistics M. 2019;42(4):1157–66.
48. Hawkes AG. Biometrika. Biometrika. 1971;58(1):83.
49. Malmgren RD, Stouffer DB, Campanharo AS, Amaral LA. Science. 2009;325(5948):1696–700.
50. Marshall AD, Compagno LJV, Bennett MBZ. Zootaxa. 2009;2301(1):1–28.
51. Deakos MH. Environmental biology of fishes. Environ Biol Fishes. 2012;94(2):443–56.
52. Stevens GMW. Conservation and population ecology of manta rays in the Maldives. York, England, UK: University of York; 2016.
53. Alstott J, Bullmore E, Plenz DP. PLoS ONE. 2014;9(1):e85777.
54. Yang Y, Foster KR, Coyte KZ, Li A. Nature Ecol Evol. 2023;7(10):1610–9.
55. Mourier J, Lédée EJI, Jacoby DMP. bioRxiv. 2019;749085.
56. Wu J, Yu Y, Ren G. Fractal Fract. 2024;8(5).
57. Sugihara G, May R, Ye H, Hsieh CH ao, Deyle E, Fogarty M, et al. Science. 2012;338(6106):496–500.
58. Campo-Bescós MA, Muñoz-Carpena R, Kaplan DA, Southworth J, Zhu L, Waylen PR. PLOS ONE. 2013;8(8):1–14.
59. Li J, Convertino MP. PLOS ONE. 2021;16(10):1–43.
60. Rinaldo A, Gatto M, Rodriguez-Iturbe I. Adv Water Res. 2018;112:27–58.
61. Pianosi F, Beven K, Freer J, Hall JW, Rougier J, Stephenson DB, et al. Environ Model Softw. 2016;79:214–32.